

Experimental generation of arbitrarily shaped diffractionless superoscillatory optical beams

Elad Greenfield,^{1,*} Ran Schley,¹ Ilan Hurwitz,¹ Jonathan Nemirovsky,¹ Konstantinos G. Makris,² Mordechai Segev²

¹Physics Department and Solid State Institute, Technion, Haifa 32000, Israel

²Department of Electrical Engineering, Princeton University, Princeton, NJ, 08544, USA

*Eladgr@rx.technion.ac.il

Abstract: We present, theoretically and experimentally, diffractionless optical beams displaying arbitrarily-shaped sub-diffraction-limited features known as superoscillations. We devise an analytic method to generate such beams and experimentally demonstrate optical superoscillations propagating without changing their intensity distribution for distances as large as 250 Rayleigh lengths. Finally, we find the general conditions on the fraction of power that can be carried by these superoscillations as function of their spatial extent and their Fourier decomposition. Fundamentally, these new type of beams can be utilized to carry sub-wavelength information for very large distances.

©2013 Optical Society of America

OCIS codes: (260.1960) Diffraction theory; (070.7345) Wave propagation; (070.3185) Invariant optical fields.

References and links:

1. A. Lipson, S. G. Lipson, and H. Lipson, *Optical Physics* (Cambridge University Press, Cambridge; New York, 2011).
2. G. T. di Francia, "Supergain antennas and optical resolving power," *Nuovo Cim.* **9**(S3), 426–438 (1952).
3. Y. Aharonov, D. Z. Albert, and L. Vaidman, "How the result of a measurement of a component of the spin of a spin-1/2 particle can turn out to be 100," *Phys. Rev. Lett.* **60**(14), 1351–1354 (1988).
4. M. V. Berry, "Faster than Fourier," in *Quantum Coherence and Reality; in Celebration of the 60th Birthday of Yakir Aharonov* (J. S. Anandan and J. L. Safko, Eds.) World Scientific, Singapore, pp 55–65 (1994).
5. M. V. Berry and M. R. Dennis, "Natural superoscillations in monochromatic waves in D dimensions," *J. Phys. A* **42**(2), 022003 (2009).
6. M. R. Dennis, A. C. Hamilton, and J. Courtial, "Superoscillation in speckle patterns," *Opt. Lett.* **33**(24), 2976–2978 (2008).
7. J. Baumgartl, S. Kosmeier, M. Mazilu, E. T. F. Rogers, N. I. Zheludev, and K. Dholakia, "Far field subwavelength focusing using optical eigenmodes," *Appl. Phys. Lett.* **98**(18), 181109 (2011).
8. M. Mazilu, J. Baumgartl, S. Kosmeier, and K. Dholakia, "Optical eigenmodes; exploiting the quadratic nature of the energy flux and of scattering interactions," *Opt. Express* **19**(2), 933–945 (2011).
9. F. M. Huang, Y. Chen, F. J. G. de Abajo, and N. I. Zheludev, "Optical super-resolution through superoscillations," *J. Opt. A, Pure Appl. Opt.* **9**(9), S285–S288 (2007).
10. F. M. Huang and N. I. Zheludev, "Super-resolution without evanescent Waves," *Nano Lett.* **9**(3), 1249–1254 (2009).
11. E. T. F. Rogers, J. Lindberg, T. Roy, S. Savo, J. E. Chad, M. R. Dennis, and N. I. Zheludev, "A super-oscillatory lens optical microscope for subwavelength imaging," *Nat. Mater.* **11**(5), 432–435 (2012).
12. E. T. F. Rogers, S. Savo, J. Lindberg, T. Roy, M. R. Dennis, and N. I. Zheludev, "Super-oscillatory optical needle," *Appl. Phys. Lett.* **102**(3), 031108 (2013).
13. K. G. Makris and D. Psaltis, "Superoscillatory diffraction-free beams," *Opt. Lett.* **36**(22), 4335–4337 (2011).
14. J. Durnin, J. J. Miceli, and J. H. Eberly, "Diffraction-free Beams," *J. Opt. Soc. Am. A* **3**, 128–P128 (1986).

Introduction

The diffraction limit, first defined by Ernst Abbe in 1873, is a fundamental limit on the diffractive imaging resolution of optical systems [1]. This is the fundamental constraint on the smallest spot into which a light beam can be focused by an optical system. The diffraction limit is determined by the extent of spatial spectrum of the beam – that is, by the fastest-

oscillating Fourier component of the optical field. This constraint has far reaching implications ranging from the maximum attainable resolution with optical diffractive microscopy, to the limit on the accuracy of laser machining processes. Essentially, the diffraction limit reflects the fundamental Fourier-Heisenberg uncertainty principle. However, already in 1952, Toraldo di Francia [2] noted that this limit does not impose a constraint on smallest-achievable localized spot of light for an optical system of given numerical aperture. Decades later, Yakir Aharonov et al. published several pioneering papers on the seemingly unrelated problem of quantum measurements [3], and soon thereafter Michael Berry brought the concept into the general domain of waves, and started the research direction now termed superoscillations [4]. Berry explored superoscillatory functions, which, in finite, yet arbitrarily large regions of space oscillate faster than the fastest (highest) Fourier component of the entire function. Such superoscillations occur naturally in optics near optical phase singularities [5] or in random optical speckle patterns [6], wherever the local gradient of the phase of the field exceeds the maximum Fourier component of the spectrum of the entire field. Further, it is possible to design superoscillatory optical fields. The idea of using superoscillations for sub-diffraction limited light focusing [2,7,8] and even subwavelength super-resolution imaging [9–11] has been successfully proven in experiments. However, these methods generally produce a field with superoscillatory features occurring in a single plane of propagation, while moving away from this plane causes very quick broadening, typically within a propagation distance of few wavelengths. Notwithstanding the great potential of applying superoscillations to super-resolution imaging [11,12], the quick spreading of these super-oscillatory “speckles” makes them inapplicable in a wide range of situations, such as, for example, for optical manipulation of small particles over long trajectories, or for phase imaging of thick biological samples. Also important, the very rapid spreading of optical superoscillations generated through current techniques makes them unusable for encoding and transmitting sub-wavelength information carried upon the propagating beam, which is a conceptually important prospect for applications of superoscillatory beams in information sciences. Although [12] demonstrates a focal spot that is extended in the axial direction considerably beyond what was shown earlier, this focal spot in [12] was not designed to be non-diffracting for large distances, hence it indeed broadened within a few wavelengths of propagation away from the focal plane.

Clearly, for some time, it seemed that superoscillatory beams are fundamentally doomed to fade away through diffraction broadening at a rate that would severely limit their usefulness. However, two years ago Makris and Psaltis [13] introduced a conceptually important idea, demonstrating ‘superoscillatory shape-preserving beams’. Using a superposition of shape-preserving ‘Bessel beams’ [14] of different orders but of the same transverse wavenumber, the authors of [13] showed that it is theoretically possible to generate non-broadening optical beams incorporating sub-diffraction-limited features. However, to the best of our knowledge, non-diffracting superoscillations have never been generated experimentally. Further, although in essence the method in [13] can be used to design any arbitrarily shaped diffractionless superoscillatory pattern, it would require solving an infinite number of equations simultaneously to achieve this goal.

Here, we present the first experiments on nondiffracting optical superoscillations. We demonstrate theoretical and experimental control over the shape, size, and spatial orientation of sub-diffraction-limited features, and demonstrate their transmission for long distances without ‘smearing’ due to diffraction broadening. Our beams display arbitrarily small superoscillatory features with a predetermined field distribution. We experimentally design beams having ‘line-shaped’ superoscillatory features as small as 14% of the diffraction limit of our system, and having negligible diffraction broadening over propagation distances as long as 250 Rayleigh lengths. Importantly, we demonstrate versatile control over the features of these beams, both in theory and experiment: we control the width, and rotational orientation of the line-shaped superoscillations at will. In addition, we derive a general analytic

methodology for generating arbitrarily-shaped nondiffracting superoscillatory optical beams. Our derivation ultimately results in analytic expressions, hence in contrast to the method in [13], it facilitates arbitrary shaping of the beams without the need for solving **any** equations at all. Last, we explore the power-transmittance efficiency of the sub-diffraction limited features, as function of their spatial extent, feature size, and Fourier decomposition. We present general conditions for generating arbitrarily shaped superoscillations approximating a known function in space to finite Taylor and/or Fourier expansion order. The spatial extent of the superoscillation, and the quality of the arbitrary shaping come at the expense of the power transmitted with the diffractionless superoscillatory feature. The method we present is general, allowing straight forward engineering of diffractionless superoscillations with predesigned parameters. As examples, we design arrays of diffractionless superoscillations shaped as sinusoidal and rectangular waveforms.

Methodology

We begin by considering a distribution of a superposition of optical Bessel beams of different orders, which in general can be mutually shifted from one another in the plane transverse to the optical axis. The complex optical field amplitude $E(r,z)$ is

$$E(r, \theta, z) = e^{-ikz} \sum_{m=0}^N \sum_{l=0}^{l(m)} a_{lm} J_m(k_r |r - r_{lm}|) e^{-im\theta_m}, \quad (1)$$

We use a cylindrical coordinate system (r, θ, z) depicted in Fig. 1. The field amplitude $E(r, \theta, z)$ comprises Bessel beams of order 0 to m . There can be an arbitrary number of beams for each order m ($l(m)$). The m^{th} order beam of index $l(m)$, J_{lm} , is centered around $|r_{lm}|$. All of the beams share the same transverse wave number, k_r . For each laterally shifted coordinate system, the angular coordinate is denoted as θ_{lm} . The coordinate system is depicted in Fig. 1(a). Since each Bessel beam is propagation-invariant (independent of the axial coordinate z), and since all of the beams acquire phase with the same rate, as they propagate along z , their superposition is propagation-invariant as well.

Before we present the general approach to shaping of this field, consider an example for a superposition of two 2nd order beams, with $m = 2$, $l = 2$ in Eq. (1). Their centers can be arbitrarily set on the x axis, and their relative phase can be set to π , with the resulting field amplitude along the x axis

$$E(x, z) = a_{21} J_{21}(k_r x) e^{-ikz} - a_{22} J_{22}(k_r (x - x')) e^{-ikz}, \quad (2)$$

where a_{21}, a_{22} , and k_r are real and positive constants.

For small distances $x < 1/k_r$ and lateral separations between these beams, $|x - x'| < 1/k_r$, Eq. (2) can be approximated to

$$E(x, z) \cong \frac{e^{-ikz}}{2!} \left[a_{21} \left(\frac{k_r x}{2} \right)^2 - a_{22} \left(\frac{k_r (x - x')}{2} \right)^2 \right]. \quad (3)$$

For $a_{22} > a_{21}$, $E(x,z)$ has a maximum at $x_{\text{max}} = x' \cdot a_{22} / (a_{22} - a_{21})$, and crosses zero at $x = \sqrt{a_{22} x'} / [\sqrt{a_{22}} - \sqrt{a_{21}}]$ and at $x = \sqrt{a_{22} x'} / [\sqrt{a_{22}} + \sqrt{a_{21}}]$. Hence, the optical intensity has a single arbitrarily small feature of width $\Delta x = 2\sqrt{a_{22} a_{21} x'} / [a_{21} - a_{22}]$ between these two zeros. This feature can be made arbitrarily small since x' can be made arbitrarily small, at the expense of the reduction in the power carried by this feature. Namely, since $E(x_{\text{max}}) \sim (x')^2$,

the peak intensity scales as $I(x_{\max}) \sim (x')^4$, and the power (per unit length in the y direction) carried by this small feature during propagation along the z direction scales as $P \sim (x')^5$. This is, of course, only one particular example of the general trend [4] that the optical power carried within superoscillatory features decays with decreasing feature size.

Experimental

We realize the above example experimentally in the apparatus sketched in Fig. 1. Two plane waves emerging from the same laser (HeNe, $\lambda = 633\text{nm}$) propagate in the z direction, illuminating a phase mask. The mask carries the phase $m\theta$, where θ is the angle in polar coordinates in the plane of the mask, and m is generally an integer. In this example $m = 2$. The Axicon in our system has a base angle of 2° and a refractive index ~ 1.48 , hence a light ray incident perpendicularly exits the Axicon with an angle of $\sim 0.96^\circ$. The numerical aperture (NA) of our system is thus 0.0168. The diffraction limit of our system, given by $\lambda / (2 \cdot \text{NA})$, is roughly $19\mu\text{m}$. The beams are laterally shifted from one another and superimposed before passing through a conical lens (axicon). At the output of the lens, the beams approximate two laterally shifted 2nd order Bessel beams with complex field amplitudes $E_1 = A_{21} e^{i(m\theta - kz)} J_2(k_r r)$, and $E_2 = A_{22} e^{i(m\theta - kz)} J_2(k_r (r - r'))$ respectively. The complex coefficients A_{21} and A_{22} are set by attenuators and by choosing the relative phase between the beams in the apparatus. The field is made identical to the field in Eq. (3) along the x -axis, by choosing $A_{22} = a_{22}$; $A_{21} = e^{i\pi} \cdot A_{22} / 10$. Since k_r is set solely by the axicon's focal power, the resulting diffraction pattern is non-broadening to large distances, limited only by the diameters of the conical lens and of the beams. Alignment of the beams in this setup is easily controllable. Angular misalignment of the beams with respect to one another results in the broadening or focusing of the superoscillation as it propagates, where the angle of focusing or broadening scales linearly with the angle of misalignment. As a matter of fact, this degree of freedom can be used to 'intentionally misalign' the beams, generating a superoscillation which varies its width as it propagates to a known degree. With respect to lateral misalignment of the beams, the superoscillation's width scales roughly linearly with the lateral displacement of the beams. This degree of freedom is also easy to control in our system. Controlling the relative phase between the beams to sub-micrometer scale is essential in this apparatus, since on-axis jitter of the beams relative to one another may cause unwanted destructive interference of the beams. A way to avoid this problem is to use a thick phase mask, and just one arm of the apparatus: then it is possible to superimpose the Bessel beam with its own optical 'ghost' generated by reflection within the thick phase mask. Tilting the mask with respect to the direction of the incoming beam can provide sensitive control over the lateral shift between the beams.

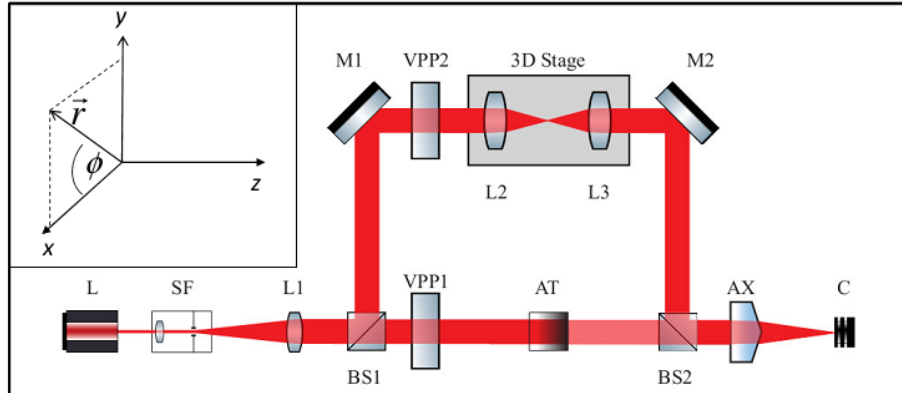


Fig. 1. Schematic of the experimental setup (not to scale). A continuous wave laser beam is spatially filtered (spatial filter 'SF') and is subsequently broadened and re-collimated, and then split in two, each separate branch acquiring a spiral phase $m\phi$ when passing through phase plate 'VPP1', VPP2. The lower branch passes through an attenuator ('AT') which sets the ratio of intensities between the beams. The upper branch can be laterally shifted in the xy plane using a telescopic system mounted on a 3D micrometric stage. The beams are recombined and pass through an axicon 'AX'. The resultant two Bessel beams are then superimposed to give a superoscillatory non-broadening beam. The beam is measured with a camera ('C') equipped with a microscope objective. The camera can slide along the z -axis, obtaining images of the xy shape of the beam at different propagation planes. Inset: Coordinate system used throughout this paper.

The experimental results, constituting the first demonstration of non-diffracting optical superoscillations, are presented in Figs. 2 and 3. Figure 2 shows the asymmetric superposition of 2nd order Bessel beams (Eq. (3)), which is shaped like a line. We vary the lateral shift between the beams (x') and hence Δx , with a simple micrometer, thus varying the width of the superoscillatory line-feature. The size can be accurately and continuously varied from 10%-50% of the diffraction limit of the system, D (Fig. 2 and inset). The peak intensity of the superoscillatory feature decays with the 4th power of its width, in accordance with the predictions above.

We now demonstrate experimental control over the properties of the superoscillatory features. In Fig. 3(a), we present the rotation of the superoscillatory feature by arbitrarily rotating the x -axis connecting the centers of the two 2nd order Bessel beams in the xy plane. In Fig. 3(b)-3(c), we show that this beam is indeed shape-preserving: the Superoscillatory feature stays perfectly intact, maintaining its widths, while propagating for distances of over 250 Rayleigh lengths.

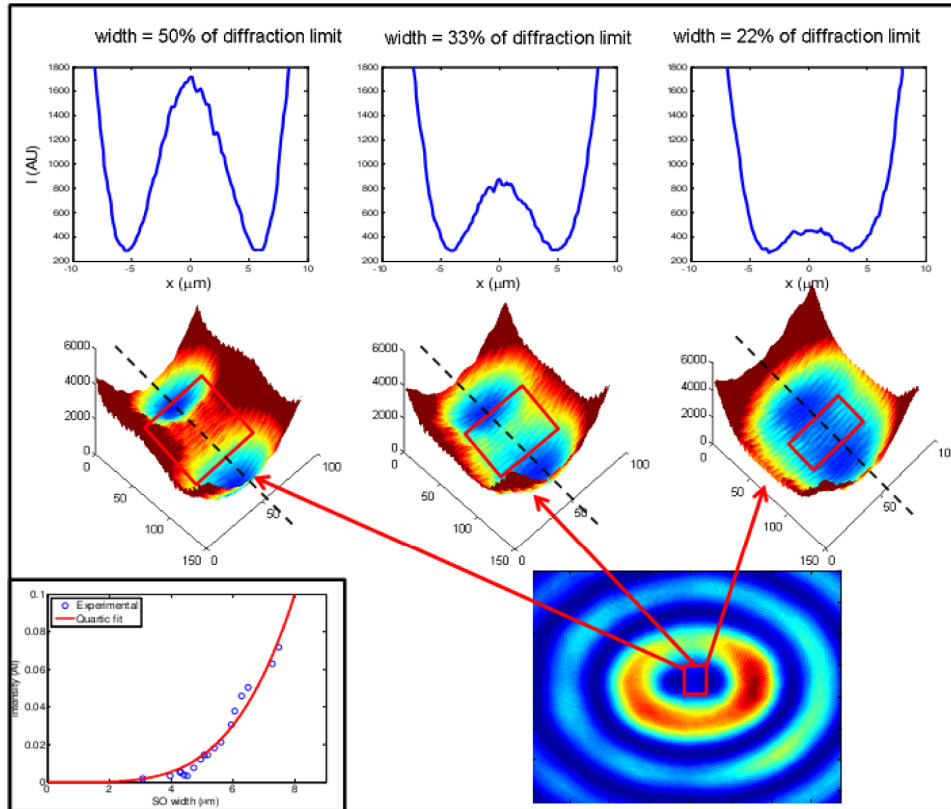


Fig. 2. Experimental demonstration of optical shape-preserving beams having sub-diffraction-limited superoscillatory (SO) features. An asymmetric superposition of 2nd order Bessel beams (whose intensity distribution transverse to the propagation direction is shown at the lower right corner) exhibits line-shaped superoscillatory features. The intensity distributions of three such superoscillations are magnified and presented in 3D layouts surrounded with red rectangles on top. One dimensional cross sections of these superoscillations along the black dashed lines are presented above the 3D plots. The presented features (whose RMS width is as small as $4\mu\text{m}$) are significantly smaller than the diffraction limit of the system, $19\mu\text{m}$. Features as small as $2.5\mu\text{m}$ were also measured (see inset). We demonstrate control over the width of the feature, decreasing it from 50% (upper left) and down to 20% (upper right) of the diffraction limit. The intensity of the features decays accordingly. Inset: Power carried by the superoscillatory feature, exhibiting decay with the 4th power of its width, in accordance with our analytic derivation.

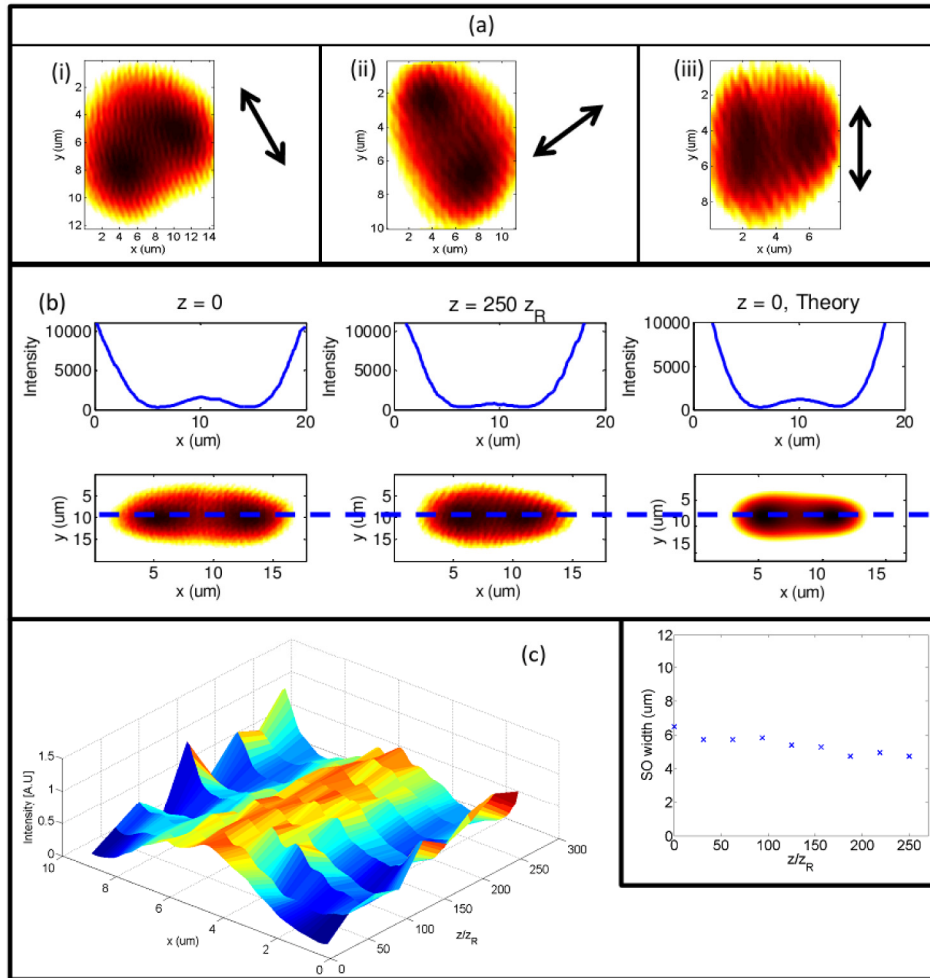


Fig. 3. (a) Experiments displaying designed rotation of an elongated superoscillation at three different orientations, (i-iii). The black arrows mark the direction of the long dimension of the superoscillation. (b) Shape-preserving propagation of the superoscillatory feature: The feature is measured at $z = 0$ (left) and after propagating 250 Rayleigh lengths (Z_R) (middle), maintaining its width while propagating. The lower images are 2D intensity distributions of the superoscillatory features, and the graphs above them are intensity cross-sections of those distributions, taken along the blue dashed line. The propagation dynamics show good agreement with theoretical prediction (right). (c) Detailed propagation dynamics, showing the cross-section of the superoscillation as it propagates along the propagation axis for 250 Rayleigh lengths. The beam intensity is normalized to unity at each plane for clarity of observation. Inset: width of the superoscillation between its zeros, as function of propagation distance – exhibiting almost a flat dependence. The superoscillations exhibits some minor focusing as it propagates, due to slight angular misalignment of the beams.

Arbitrarily shaped superoscillations

We now introduce a general approach for generating arbitrarily shaped non-broadening superoscillatory beams using superpositions of high order Bessel beams. For this we consider the field comprising a superposition of superoscillations as before, but we limit our derivation to the case where the centers of all of the beams are set at the origin. This also inevitably introduces another simplification to the field in Eq. (1), since all l instances of a m^{th} order Bessel beam are now degenerate, and the field can now be written as

$$E(r, z) = e^{-ikz} \sum_{m=0}^N a_m J_m(k_r r) e^{-im\theta} \quad (4)$$

In [13], Makris and Psaltis showed that, in this case, it is possible to tailor the positions of the zeros and finite values of the field at any point in the $r - \theta$ plane. In essence the method in [13] can hence be used to generate arbitrary shaped superoscillatory beams. However, in practice this would require simultaneously solving an infinite number of equations. In contrast, we take a different approach, deriving analytic solutions that allow generation of nondiffracting superoscillations with any predetermined shape, **without the need for equation-solving at all**. Choosing as before the axis of the superoscillation as x , we approximate the field in Eq. (4) for $x \ll 1/k_r$, which is always the case when considering sub-diffraction limited features. The field along the x -axis is

$$E(x, z) = \sum_{m=0}^{m=N} a_m \sum_{s=0}^{\infty} \frac{(-1)^s}{s!(m+s)!} \left(\frac{k_r x}{2} \right)^{m+2s} = e^{-ikz} \sum_{j=0}^{\infty} \left(\sum_{k=0}^{j/2} \frac{(-1)^k a_{j-2k}}{k!(j-k)!2^j} \right) (k_r x)^j, \quad (5)$$

where we set $a_{j-2k} = 0$ for $j - 2k > N$ and for $j - 2k < 0$.

We approximate each coefficient of the j^{th} order polynomial term x^j in Eq. (5) to include only the contribution from the highest order coefficient a_j ($k = 0, s = 0$). For instance, we approximate the coefficient for the parabolic term $\left(\frac{a_2}{8} - \frac{a_0}{4} \right) (k_r x)^2 \sim \left(\frac{a_2}{8} \right) (k_r x)^2$ and for the cubic term $\left(\frac{a_3}{48} - \frac{a_1}{16} \right) (k_r x)^3 \sim \left(\frac{a_3}{48} \right) (k_r x)^3$, arriving at

$$E(x, z) \cong e^{-ikz} \sum_{m=0}^{m=N} \frac{a_m}{m!} \left[\frac{k_r x}{2} \right]^m. \quad (6)$$

This approximation is justified, since, as we show below, the coefficients a_m grow exponentially with m . Numerical comparison between superoscillations designed using Eq [5], or through its approximated version - Eq [6], are presented in Fig. 4, showing that for all practical purposes, these two forms are only negligibly different from one another.

To design an arbitrarily shaped superoscillatory optical field whose complex amplitude follows the function $f(x)$, at least on the x -axis, we expand the field in a Taylor series,

$$f(x) = \sum_m b_m x^m, \quad m=0,1,2,\dots \quad (7)$$

Matching the coefficients of Eq. (6) to those of the Taylor expansion, Eq. (7), an arbitrarily shaped superoscillation can be generated if the amplitudes a_m are set to

$$a_m = \frac{m! b_m 2^m}{[k_r]^m}. \quad (8)$$

Hence, the complex field amplitude for a field realizing a superoscillatory feature $f(x)$ can be generated as a superposition of Bessel beams, such as

$$E(x, z) = e^{-ikz} \sum_{m=0}^{m=N} \frac{m! b_m 2^m}{[k_r]^m} J_m(k_r x). \quad (9)$$

Equation (9) is a particularly intuitive representation of the field, which shows some quantitatively useful properties. The Bessel beam of order m contributes the m^{th} order term of the Taylor's expansion to the desired superoscillatory field. Hence, it is clear that higher order

Bessel beams are required for extending the spatial support of the superoscillatory region of these non-broadening wavepackets. However, Eq. (9) also includes multiplication of the m^{th} order beam by 2^m , hence the ratio between the peak intensity at the superoscillatory region, henceforth denoted I_{SO} , and the peak intensity of the beam outside the superoscillatory region, (which is also the peak intensity of the entire beam, henceforth denoted I_{beam}) scales as

$$R \equiv I_{SO} / I_{beam} \sim 2^{-2N}. \quad (10)$$

For a beam of constant given power, R is roughly a measure of the fraction of power that can be carried by the superoscillatory region of the propagation-invariant beam. It is then apparent that extending the spatial support of the superoscillation requires higher orders of the Taylor expansion for $f(x)$, and this comes at the expense of an exponential decrease in the power the superoscillation. Furthermore, shrinking the entire superoscillatory region (approximated by the m^{th} order Taylor's series) by a factor of r increases k_r by a factor r^m , and hence decreases the powers ratio R by a factor of r^{-2m} .

We demonstrate these ideas theoretically with an array of sinusoidally and rectangularly-shaped (Figs. 4(a)-4(b)) shaped non-broadening superoscillations. The superoscillation precisely matches the pre-designed shape $f(x) = \sin(\alpha x)$ for $m \rightarrow \infty$. Given the constraints imposed by Eq. (10), this implies that the power carried by the superoscillatory region of the field becomes vanishingly small as m increases. Figure 4(a) shows the generation of two sinusoidal superoscillations. Here we calculate the superposition of Bessel beams up to order 3. Extending the superoscillatory region to have 6 superoscillations (Fig. 4(b)) requires 19 orders of the Taylor series of the sinusoidal waveform, hence a Bessel beam superposition up to order 19.

For practical applications, encoding and transmitting a train of superoscillatory rectangular 'bits' in a non-broadening beam may be of importance. However, the polynomial (Taylor series) basis may be inconvenient for generation of such features. We demonstrate that a Fourier decomposition can be used, leading to a superoscillation with a field distribution closely matching a rectangular-pulse train. In this case, $f(x)$ is a rectangular waveform with a period of length L . We expand this waveform in a sine-series, and each sine in a Taylor series, to obtain

$$f(x) = \sum_{n=1,3,5,\dots} c_n \sin\left(\frac{2n\pi}{L}x\right) = \sum_{n=1,3,5,\dots} \frac{4}{\pi n} \sum_{k=0}^{\infty} \frac{(-1)^k}{(2k+1)!} \left(\frac{2n\pi x}{L}\right)^{2k+1} = \sum_{k=0}^{\infty} b_{2k+1} x^{2k+1} \quad (11)$$

Hence, the coefficient for the $(2k+1)^{\text{th}}$ order Bessel beam is

$$b_{2k+1} = \sum_{n=1,3,5,\dots} \frac{4}{\pi n} \frac{(-1)^k}{(2k+1)!} \left(\frac{2n\pi}{L}\right)^{2k+1}, \quad (12)$$

And the optical field, in this case, is

$$\begin{aligned} E(x, z) &= e^{-ikz} \sum_{k=1,3,5,\dots}^N \frac{k! b_k 2^k}{[k_r]^k} J_k(k_r x) = \\ &= \sum_{k=1,3,5,\dots}^N \frac{k! 2^k}{[k_r]^k} \sum_{n=1,3,5,\dots} \frac{4}{\pi n} \frac{(-1)^k}{(2k+1)!} \left(\frac{2n\pi}{L}\right)^{2k+1} J_k(k_r x) \end{aligned} \quad (13)$$

This example is particularly insightful, since the dependence of the power carried by the superoscillatory region is separately dependent on the spatial 'sharpness' of the superoscillation, given by the Fourier order n , and the superoscillation's spatial support, indicated by the Taylor order k . Namely, for spatial support given by a known highest order

in the Taylor series k , the power scales roughly as $b_{2k+1} = \sum_{n=1,3,5,\dots} (n)^{2k+1}$. Although our work

allows versatile design of sub-diffraction-limited non-diffracting optical features that are in principle suitable for encoding and transmitting information for long distances, the strong decay of the power transmitted in the superoscillation (with increasing spatial extent and sharpness – necessitating high Taylor and Fourier components respectively) may ultimately render the whole idea of using superoscillations for long-range transmission of sub-diffraction-limit information impractical.

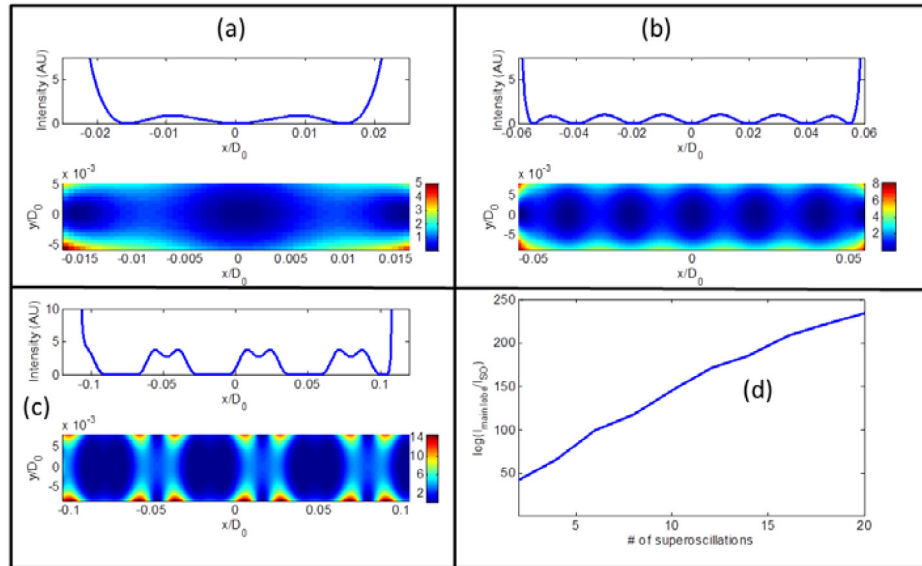


Fig. 4. Designing non-diffraction superoscillations with pre-determined shapes. (a) Setting $f(x) = \sin(ax)$, ' a ' being a constant, we construct a beam with two sinusoidal intensity features, each of width $\sim D_0 / 7$, D_0 being the diffraction limit of the system. Here the superposition is of Bessel Beams up to $m = 3$. The lower graph shows the 2D intensity distribution, and the upper graph is its horizontal cross-section. (b) Extending the spatial support of the superoscillatory region to include 6 sinusoidal superoscillations requires superposition of Bessel beams up to order 19. (c) Generating a rectangular array of superoscillatory features through superposition of Bessel beams up to order 80, and Fourier decomposition of $f(x)$ up to order 3. (d) Ratio between the peak intensity of the beam to the intensity of the superoscillatory region, as a function of the spatial support of the superoscillatory region. This dependence is roughly exponential, as expected.

Discussion and conclusion

Our work brings the concept of non-broadening superoscillatory optical beams from theory to the lab, presenting new types of superoscillatory shape-preserving beams of high versatility. Our beams feature control over new degrees of freedom, such as asymmetry and rotational orientation. Our general methodology makes it possible to design any predesigned superoscillatory non-broadening optical field in an arbitrary large regions of space, and to predesign important relevant parameters such as the power it carries. The versatility of these new beams promotes new opportunities in fields ranging from sub-wavelength phase imaging of thick, transparent biological samples, to optical manipulation of particles and fluids at the sub-wavelength scale, and subwavelength 3D optical writing. As such, we envision that this first experimental demonstration will soon prove an important tool in a range of applications,

and initiate interest in further scientific research of this type of beams –making them an active area of research.

Acknowledgments

This work was supported by the Israeli Focal Technology Area on Nanophotonics for Detection Program, and by an Advanced Grant from the European Research Council (ERC). E.G. gratefully thanks the Levi Eshkol Fellowship of the Ministry of Science, Israel. The authors thank Michael V. Berry for valuable discussions.